

## Investigation on the Influence of Plasma Properties and SOL Transport on the Particle Flux Profiles on Divertor Plates in the Large Helical Device

S. Masuzaki<sup>a\*</sup>, M. Kobayashi<sup>a</sup>, T. Morisaki<sup>a</sup>, N. Ohyaabu<sup>a</sup>, A. Komori<sup>a</sup>, Y. Feng<sup>b</sup>,

and the LHD experimental group

<sup>a</sup> National Institute for Fusion Science, Oroshi 322-6, Toki 509-5292, Japan

<sup>b</sup> Max-planck-Institut fuer Plasmaphysik, Euratom Association, D-17491 Greifswald, Germany

### Abstract

Particle flux profiles on the divertor plates and the electron temperature profiles in the scrape-off layer (SOL) in the Large Helical Device (LHD) heliotron were investigated with EMC3-EIRENE code. These profiles are modified during a discharge due to the changes of the edge plasma density and temperature those can cause the change of transport coefficient. Comparison of the edge electron temperature profiles between the measurements and the simulations revealed that the cross field transport coefficients in the LHD scrape-off layer depend on plasma parameters, especially electron temperature. For the particle flux profile on the divertor plates, the absolute value of the simulation results with the transport coefficient consistent with the edge temperature profile analysis were well agree with the experimental data, though the profile shapes of experimental data were not necessarily reproduced well by the simulation.

---

PACS: 52.25.Fi, 52.40.Hf, 52.55.Hc,

JNM keywords: Plasma Properties

PSI-18 keywords: Cross-Field Transport, Divertor plasma, Edge plasma, LHD, Stochastic boundary

\*Corresponding author address: Oroshi 322-6, Toki 509-5292, JAPAN

\*Corresponding author E-mail: masuzaki@LHD.nifs.ac.jp

Presenting author: Suguru MASUZAKI

Presenting author: E-mail: masuzaki@LHD.nifs.ac.jp

## 1. Introduction

To understand the mechanisms of determining the particle and heat flux profiles on the divertor is a crucial issue for the effective particle control and the extension of the lifetime of the divertor plates. The profiles are mainly determined by the balance of parallel and perpendicular transports to magnetic field in the scrape-off layer (SOL). In a tokamak with a poloidal divertor configuration, the magnetic field lines structure is “onion-skin” like, and the parallel transport is dominant to determine the divertor plasma properties. Therefore, divertor plasma profiles are sometimes compared with the upstream profiles by using the mapping of the profiles on the divertor plate to e.g. midplane coordinate [1]. By comparison, the magnetic field lines structure outside the last closed flux surface (LCFS) is rather complicated in the Large Helical Device (LHD) heliotron (helical coils number = 2 and toroidal mode number = 10). The intrinsic ergodic layer surrounds LCFS, and magnetic island chains are embedded in the layer. The field lines in the ergodic layer are connected to the divertor plates through the edge surface layer. The connection length of the open field lines in the ergodic layer are over several hundreds meters while the field line length from the X-point to the divertor plates is a few meters for the strong poloidal component of magnetic field in the divertor region [2, 3]. So the mapping method cannot be simply applied to the divertor plasma analysis.

Plasma transport in the LHD SOL has been investigated experimentally using Thomson scattering measurement [4] and Langmuir probes [5], and theoretically using three dimensional edge transport code, EMC3-EIRENE [6, 7]. For example, it was revealed with the simulation that the perpendicular transport is comparable to parallel transport in the LHD SOL, and counter flows induced by the ergodic field lines break the pressure conservation along flux tubes through the friction [6].

The particle flux profile on the divertor plates has been investigated using Langmuir probe arrays embedded in the plates. It was revealed that particle flux position and deposition

profile are mainly determined by the field lines structure on the plates [3]. However the detailed analysis of the particle flux profiles on the divertor plates has not been conducted.

In this paper, the transport coefficients in the LHD SOL are estimated by comparing the experimental data to the simulation results using EMC3-EIRENE code, and the particle flux profiles on the LHD divertor plates are investigated focused on the relationship between them and the edge transport coefficients.

## 2. Experimental and computational set-up

The particle flux profiles on the divertor plates vary place to place for the three dimensional structure of the LHD SOL. In this study, the inboard and the top Langmuir probe arrays were used to measure the ion saturation current, that is, the particle flux, because the particle flux profiles on them have typical structures. Figure 1(a) and (b) show schematic views of the LHD poloidal cross-sections in which located the divertor plates where are embedded the Langmuir probe array [3]. The inboard and top Langmuir probe arrays have 20 and 16 electrodes, respectively, and the spatial distance between electrodes is 6 mm. They are embedded along the edge of the divertor plates. Figure 2 (a) and (b) show the profiles of the field lines connection length ( $L_c$ ) along the probe arrays on the inboard and the top divertor plates, respectively. Horizontal axis is the position on the divertor plates, and the origin is the private side edge of the plates. As shown by these figures, these positions of the divertor plates are characteristic positions. On the inboard plate, long  $L_c$  field lines are concentrated into relatively narrow width. On the other hand, there are some long  $L_c$  field lines peaks in the profile on the top plate, and the width is larger than that on the inboard plate.

The upstream electron density and temperature profiles along the mid-plane on a horizontally elongated cross section were measured by using Thomson scattering measurement [8].

The operational magnetic configuration was as follows:  $R_{ax}$  (magnetic axis) = 3.75 m,  $B_t = 2.64$  T, the toroidal field direction is clockwise.

In order to analyze the transport in the LHD SOL, the three dimensional edge transport code, EMC3-EIRENE, has been utilized. Because of technical difficulties, the three dimensional mesh for the code did not fully include the divertor legs. To analyze the particle and heat flux profiles on the divertor plates, one dimensional fluid equations were solved using the upstream plasma parameters with the assuming no radiation loss and perpendicular transport in the divertor legs. For the short field line length between the X-point and the divertor plates, these assumptions are considered to be reasonable. In this study, impurity transport and radiation were not taken into account in the calculation.

### 3. Results and Discussion

The electron density and temperature dependences of the particle and heat flux profiles in the three discharges (#73141, 73161 and 73508) were analyzed. Figure 3 shows time evolutions of the electron density ( $n_{e,LCFS}$ ) and temperature ( $T_{e,LCFS}$ ) at LCFS during these discharges. During #73141 and #73161,  $n_{e,LCFS}$  was almost same, though  $T_{e,LCFS}$  in #73161 was about two times higher than that in #73141.  $T_{e,LCFS}$  during #73508 was almost same as that in #73141, though  $n_{e,LCFS}$  was about 6 times higher in #73508.

To estimate the cross-field transport coefficients, the comparison of electron temperature profiles in the LHD SOL between Thomson scattering measurement and simulation results was conducted as shown in Fig. 4. In the same manner as reference [6], the cross-field transport coefficients were kept spatially constant, and were assumed to be  $\chi_e = \chi_i = \chi = 3D$ . In Fig. 4, the measured profiles have steeper gradient than simulated profiles in the inner region ( $R < 4.65$  m). It was pointed out in reference [7] that the transport property should be changed at this region, and the simulation using constant cross-field transport coefficients

cannot reproduce the measured profiles in the inner and outer regions simultaneously. In this study, the cross-field transport coefficients were selected to fit the outer region. As the result of the comparison,  $(D, \chi)$  are estimated to be  $(0.125 - 0.25 \text{ m}^2/\text{s}, 0.375 - 0.5 \text{ m}^2/\text{s})$  for #73141,  $(0.5 - 1.0 \text{ m}^2/\text{s}, 1.5 - 3 \text{ m}^2/\text{s})$  for #73161 and  $(0.25 - 0.5 \text{ m}^2/\text{s}, 0.75 - 1.5 \text{ m}^2/\text{s})$  for #73508. These results suggest that the cross-field transport coefficients increase with a rise in the electron temperature, and they look also increase weakly with the increase of the electron density.

Figure 5 shows the comparison of the particle flux profiles on the inboard divertor plate between Langmuir probe measurements and simulations. In the simulations, same cross-field transport coefficients as the above analysis were applied. As shown in Fig. 2 (a), long  $L_c$  field lines are concentrated within about 4 mm, and thus both measured and simulated particle flux profiles have peaked profile. The deviation of the peak position between measurements and simulations is considered to be caused by the misalignment of the divertor plate. The values of the particle flux in the experimental results were well reproduced by the calculation. In the cases of #73161 and #73508, simulations with  $D = 0.5$  or  $1.0 \text{ m}^2/\text{s}$  and  $D = 0.25 \text{ m}^2/\text{s}$  reproduce the measured profiles, respectively. These  $D$  values are consistent with the results of the edge electron temperature profile analysis. On the other hand, in the case of #73141, simulations do not reproduce the measured profile. It seems that the peak of profile could not be detected by the Langmuir probe array in this case, and furthermore, the field lines structure could be modified by toroidal plasma current of about 20 kA.

Figure 6 shows the comparison of the particle flux profiles on the top divertor plate between Langmuir probe measurements and simulations. On this divertor plate, the profiles are not so simple as that on the inboard-side divertor plate, and the simulation looks to reproduce the measured profile only #73161 case, though the cross field transport coefficient cannot be deduced because the profiles look to be not sensitive to the coefficient. In the cases

of #73141 and #73508, the measured particle flux at the position of 0.078 m is comparable to the flux at the position of 0.036 m, while such a large peak is not observed at the right hand side of the particle flux profiles in the simulation results. Possible reasons of this difference between measurements and simulations are as follows: (1)  $E \times B$  and  $B \times \nabla B$  drift flow are not taken into account in the simulation and they could affect the profiles. In LHD helical divertor, the particle deposition asymmetry caused by  $B \times \nabla B$  drift has been observed [8]. (2) The assumption of  $\chi = 3D$  and spatial constant coefficients in the simulation could cause the difference.

#### 4. Summary

The particle flux profiles on the divertor plates in the LHD helical divertor and the edge electron temperature profiles in the LHD SOL were investigated by comparison between measurements and simulations using EMC3-EIRENE code. The electron temperature profiles in the outer region of the ergodic layer were well reproduced by EMC3-EIRENE simulation with the spatially constant transport coefficients. It was revealed that the cross field transport coefficients increase with a rise in the electron temperature. Density dependence of the coefficients seems to exist but weaker than temperature. Further investigations are necessary to understand the relationships between the coefficients and plasma parameters.

The particle flux profiles on the divertor plates are largely modified by changing plasma parameters. The simulation results well reproduce the value of the particle flux for different experimental conditions and location. To reproduce the particle flux profiles more correctly using the code, it seems to be necessary that the effects of drifts are taken into account.

#### Acknowledgement

The authors would like to thank the technical staff for their great supports. This work is

funded by NIFS06-07ULPP511 and the Grant-Aid for Scientific Research from MEXT of the Japanese government.

## References

- [1] for example, A. Kallenbach et al., Plasma Phys. Contr. Fusion **46** (2004) 431.
- [2] N. Ohyaib et al., Nucl. Fusion **34** (1994) 387.
- [3] S. Masuzaki et al., Nucl. Fusion **42** (2002) 750.
- [4] T. Morisaki et al., J. Nucl. Mater. **313-316** (2003) 548.
- [5] S. Masuzaki et al., J. Nucl. Mater. **313-316** (2003) 852.
- [6] M. Kobayashi et al., J. Nucl. Mater. **363-365** (2007) 294.
- [7] Y. Feng et al., Nucl. Fusion **48** (2008) 024012.
- [8] K. Narihara et al., Fusion Eng. Des. **34-35** (1997) 67.
- [9] S. Masuzaki et al., Fusion Sci. Technol. **50** (2006) 361.



## Figure Captions

Fig. 1: Poloidal cross-sections of LHD in which (a) the inboard and (b) the top Langmuir probe array embedded divertor plates were located. The red lines in (a) and (b) show the position of the plates.

Fig. 2: Connection length of field line ( $L_c$ ) profile on the inboard (a) and the top (b) divertor plates, respectively.

Fig. 3: Time evolutions of the electron density and temperature at LCFS during three analyzed discharges.

Fig. 4: Comparison of electron temperature profiles between Thomson scattering measurements and simulations in the torus outboard side in the LHD SOL for the analyzed discharges. Position of LCFS is  $R = 4.559\text{m}$  in the experimental condition in this study.

Fig. 5: Comparison of the particle flux profiles on the inboard divertor plate between Langmuir probe measurements and simulations.

Fig. 6: Comparison of the particle flux profiles on the top divertor plate between Langmuir probe measurements and simulations.

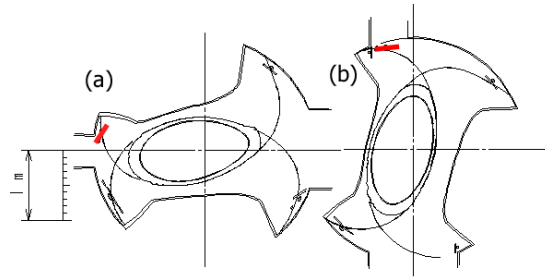


Fig.1. S. Masuzaki

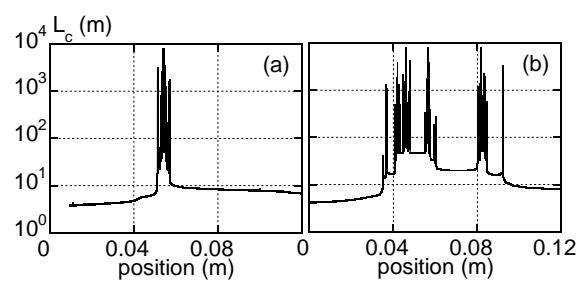


Fig. 2. S. Masuzaki

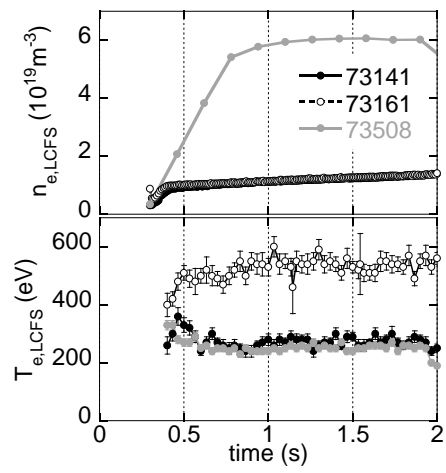


Fig. 3. S. Masuzaki

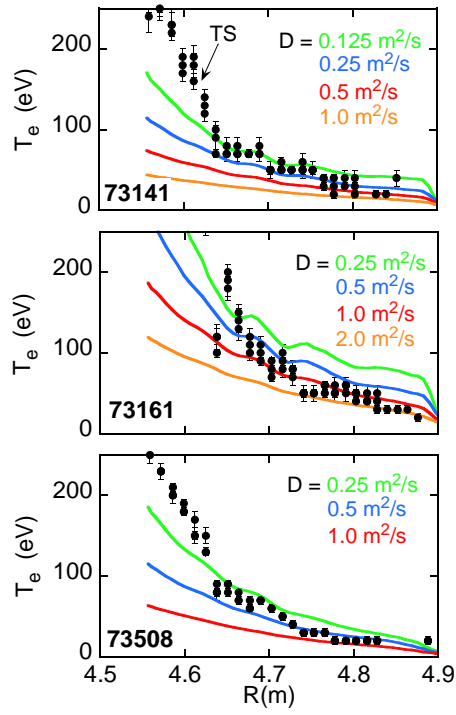


Fig. 4. S. Masuzaki

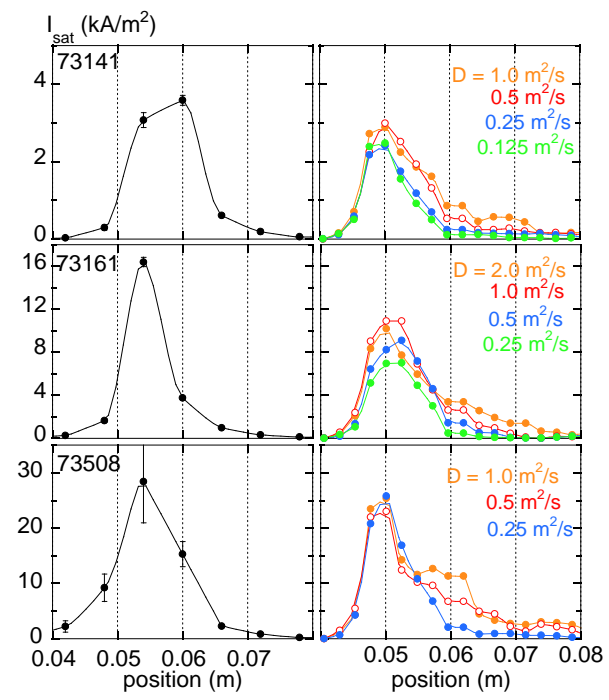


Fig. 5. S. Masuzaki

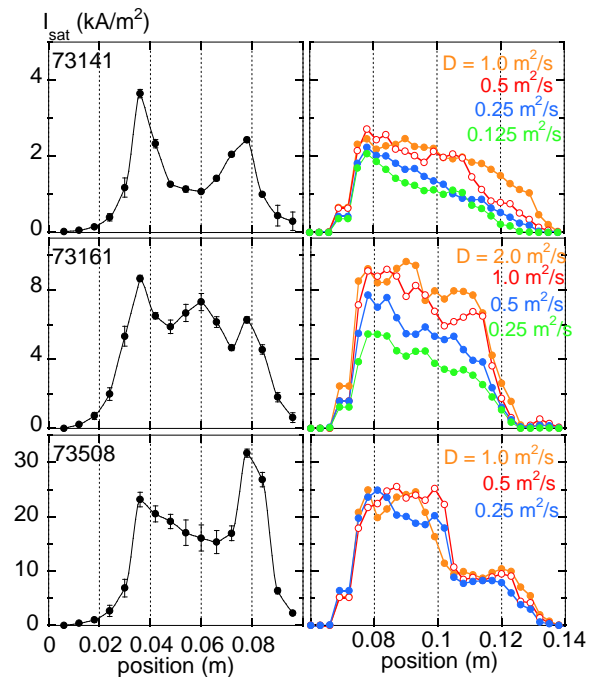


Fig. 6. S. Masuzaki